Supplementary Material:

Characterizing Changes in Drought Risk for the United States from Climate Change [1]

Kenneth Strzepek [a], Gary Yohe [b], James Neumann [c], Brent Boehlert [d]

October 12, 2010

[a] Visiting Professor
Joint Program on the Science and Policy of Global Change
Massachusetts Institute of Technology
77 Massachusetts Ave, E19-411f
Cambridge, MA 02139-4307
Phone: 617- 715-5187
Fax: 617-253-9845
E-mail: strzepek@mit.edu

[b] Woodhouse/Sysco Professor of Economics
Wesleyan University
238 Church Street
Middletown, CT 06459
Phone: 860-685-3658
Fax: 860-685-2781
E-mail: gyohe@wesleyan.edu

[c] Principal, Industrial Economics, Incorporated
2067 Massachusetts Avenue
Cambridge, MA 02140
Phone: 617-354-0074
Fax: 617-354-0463
E-mail: jneumann@indecon.com

[d] Senior Associate, Industrial Economics, Incorporated
2067 Massachusetts Avenue
Cambridge, MA 02140
Phone: 617-354-0074
Fax: 617-354-0463
E-mail: bboehlert@indecon.com

Extended Results:

Panel A of Fig. 1 in the paper text displays the geographical distribution of mean changes in the number of drought months for the SPI-12 meteorological drought index relative to the baseline for the middle 360-month period of this century (2036-2065). Panels A and B of Fig. 4S here do the same for both the SPI-5 and SPI-12 indices for all three 360-month time slices (2006 to 2035, 2036 to 2065, and 2066 to 2095). Panel A of Fig. 2 in the paper text similarly displays the geographical distribution of mean changes in the number of drought months for the extreme PDSI hydrological drought index relative to the baseline for the same 360-month period in the middle of this century. Panels C through F of Fig. 4S here do the same for mild-, moderate-, severe-, and extreme-PDSI indices for all three future time slices.

Panel B of Fig. 1 in the paper text displays geographical distributed box and whisker diagrams for each of the 99 sub-basins for changes in the number of drought months for the SPI-12 meteorological drought index relative to the baseline for the middle 360-month period of this century (2036-2065) computed from the output of every applicable GCM. Panels A and B of Fig. 5S here do the same for both the SPI-5 and SPI-12 indices for all three 360-month time slices (2006 to 2035, 2036 to 2065, and 2066 to 2095). Panel B of Fig. 2 in the paper text similarly displays geographical distributed box and whisker diagrams for each of the 99 sub-basins for changes in the number of drought months for the extreme PDSI hydrological drought index relative to the baseline for the same 360-month period in the middle of this century. Panels C through F of Fig. 5S here do the same for mild-, moderate-, severe-, and extreme-PDSI indices for all three future time slices.

The paper text also reports specific results about changes in the frequency of mild versus extreme droughts that are particularly applicable for contemplating the sustainability of agriculture in the San Joaquin Valley sub-basis of California. Fig. 6S here displays the details of time trajectories of various PDSI drought indices upon which that discussion was based.

Fig. 1S Carbon dioxide concentrations for the three selected SRES scenarios from 2000 through 2100 [1].

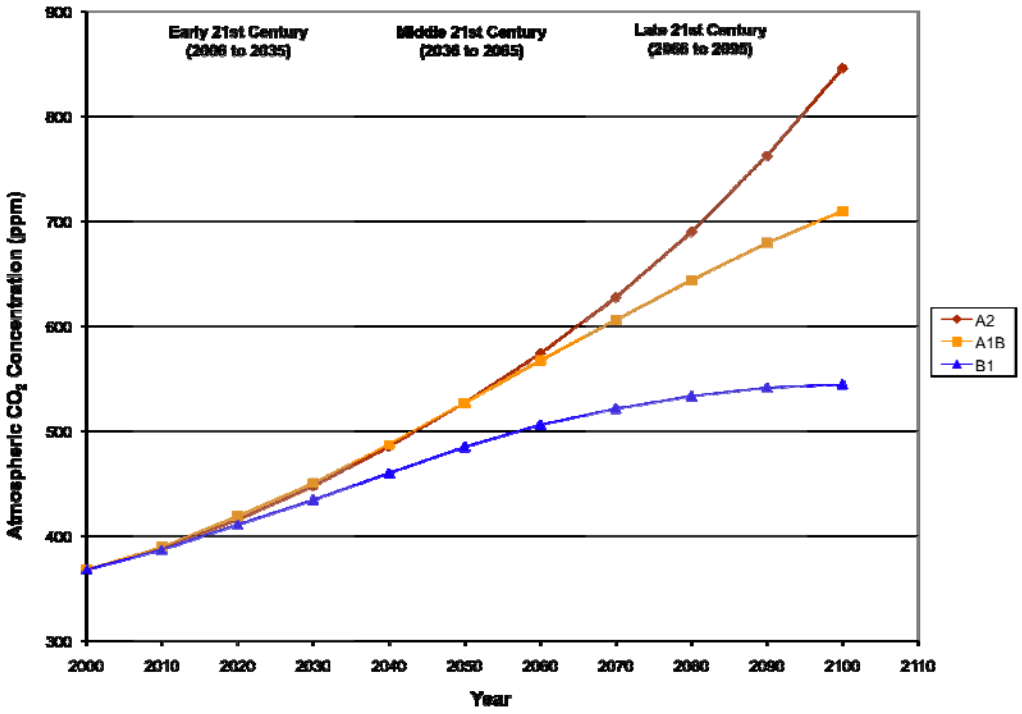

Tab. 1S Available IPCC GCM Runs for each SRES Scenario [1].

GCM	COUNTRY OF ORIGIN	SRES SCENARIO		
		B1	A1B	A2
Bjerknes Centre for Climate Research, Bergen Climate Model 2.0	Norway	✓	✓	✓
Center for Climate Modeling and Analysis, Coupled GCM 3.1	Canada	✓	✓	✓
Center for Climate Modeling and Analysis, Coupled GCM 3.1.t63	Canada	✓	✓	
Centre National de Recherches Météorologiques, Coupled Model 3	France	✓	✓	✓
Commonwealth Scientific and Industrial Research Organization, Mk 3.0	Australia	✓	✓	✓
Commonwealth Scientific and Industrial Research Organization, Mk 3.5	Australia	✓	✓	✓
Geophysical Fluid Dynamics Laboratory, Climate Model 2.0	US		✓	✓
Geophysical Fluid Dynamics Laboratory, Climate Model 2.1	US	✓	✓	✓
Goddard Institute for Space Studies, Atmospheric Ocean Model	US	✓	✓	
Goddard Institute for Space Studies, ModelEH	US		✓	
Goddard Institute for Space Studies, ModelER	US	✓	✓	✓
Institute of Atmospheric Physics, Climate Model System FGOALS G 1.0	China	✓	✓	
Institute for Numerical Mathematics, Climate Model 3.0	Russia	✓	✓	✓
Institut Pierre Simon Laplace, Climate Model 4	France	✓	✓	✓
Model for Interdisciplinary Research on Climate 3.2, High Resolution	Japan	✓	✓	
Model for Interdisciplinary Research on Climate 3.2, Medium Resolution	Japan	✓	✓	✓
Max Planck Institute for Meteorology, European Center Hamburg Model 5	Germany	✓	✓	✓
Meteorological Research Institute, Coupled General Circulation Model 2.3.2a	Japan	✓	✓	✓
National Center for Atmospheric Research, Community Climate System Model 3.0	US	✓	✓	✓
National Center for Atmospheric Research, Parallel Climate Model	US		✓	✓
UK Met Office, Hadley Center Climate Model 3	UK		✓	✓
UK Met Office, Hadley Center Global Environmental Model 1	UK		✓	✓

Fig. 2S Map of the 99 sub-basins located with the 18 2-digit HUC basins

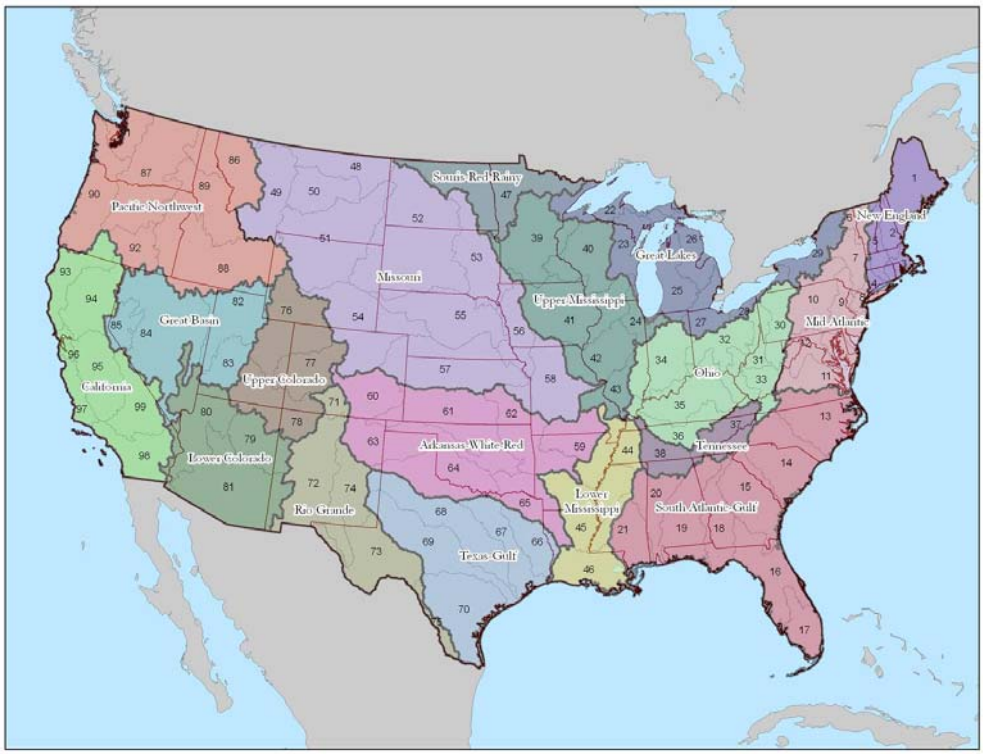

Source: USWRC 1978

Fig. 3S GCM gridcell distribution across the 99 US sub-basins.

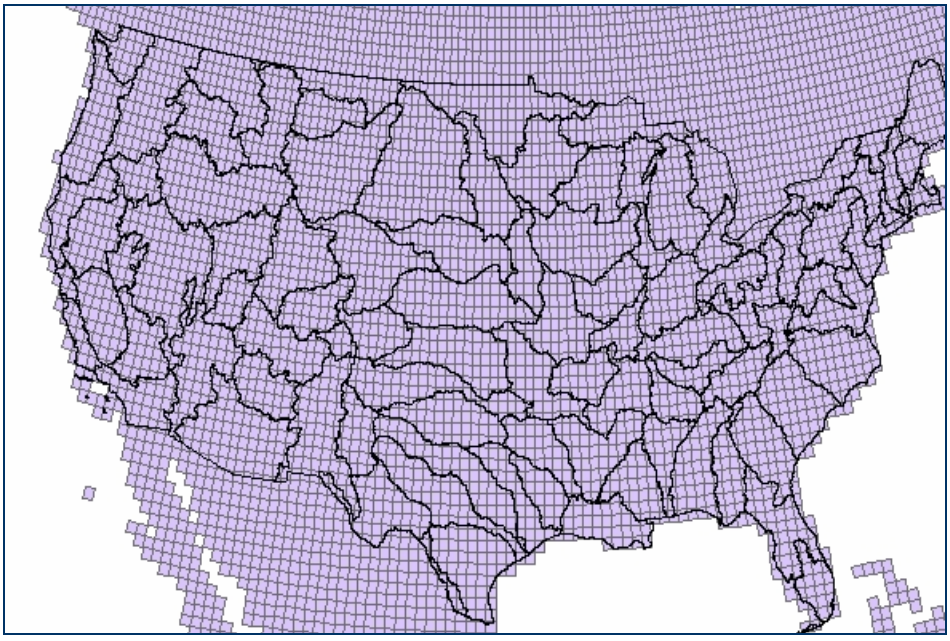

Source: USWRC 1978

Fig. 4S The geographical distribution of mean changes in the number of drought months of various indices relative to the baseline for the early, middle, and late 360-month periods of this century (2006 to 2035, 2036-2065, and 2066 to 2095) for the three SRES scenarios. Panel A – SPI-5; Panel B – SPI-12; Panel C – PDSI Mild; Panel D – PDSI Moderate; Panel E – PDSI Severe; and Panel F – PDSI Extreme.

Panel A – SPI-5. Mean results for alternative climate scenarios.

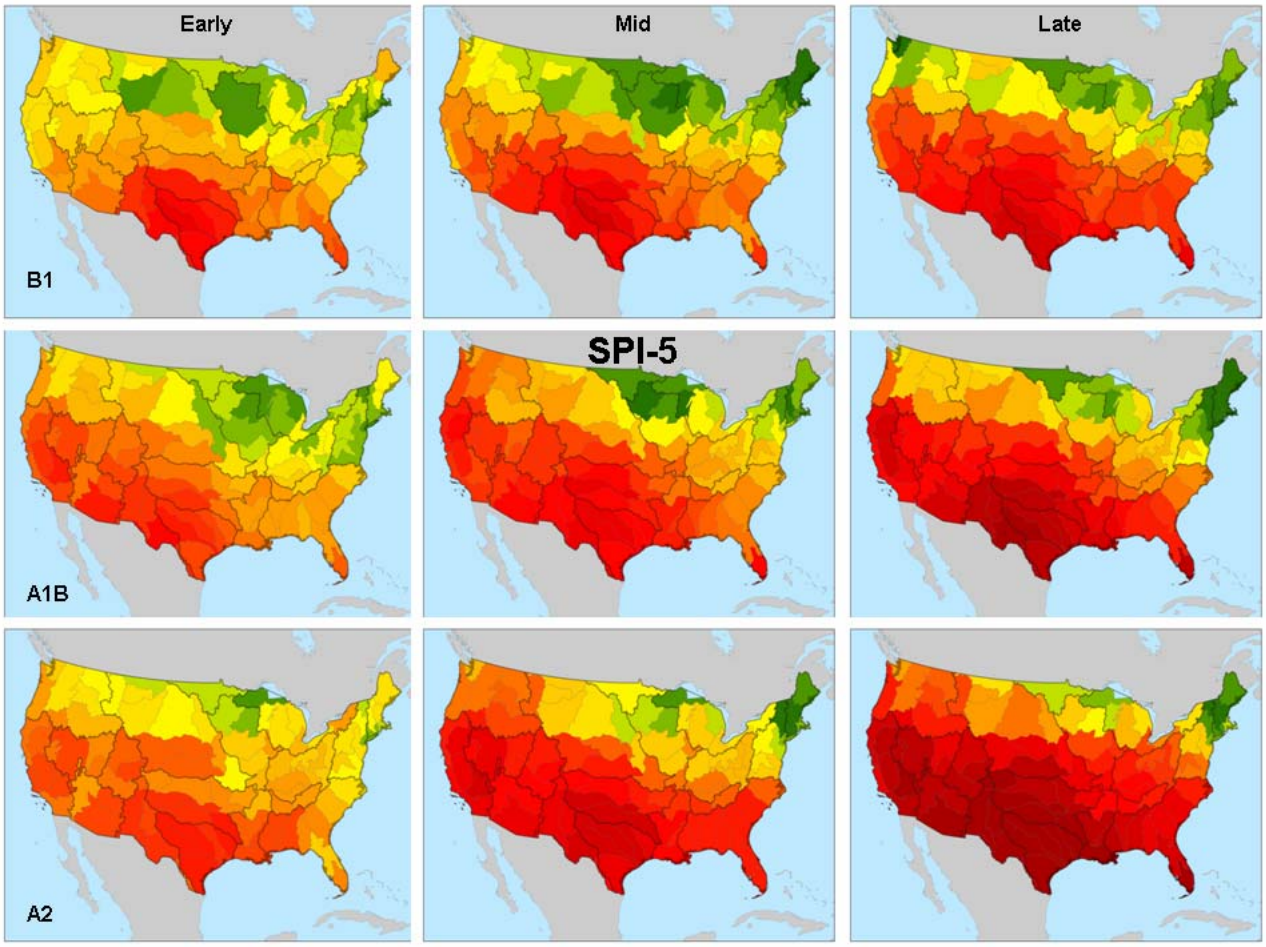

Color Scale for Figure 4, Panel A:

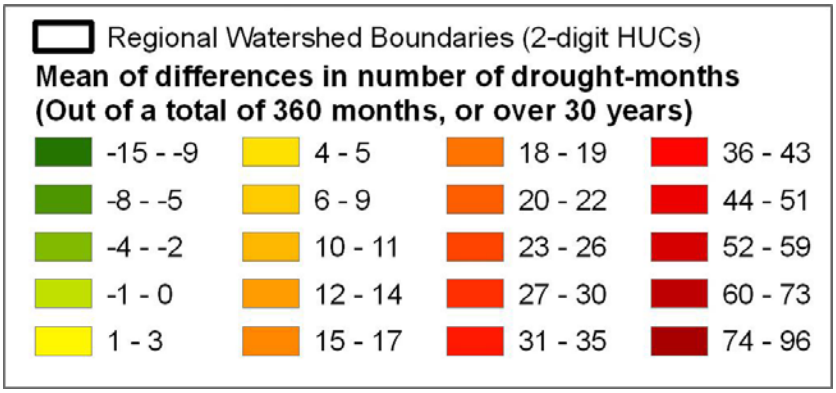

Panel B – SPI-12. Mean results for alternative climate scenarios.

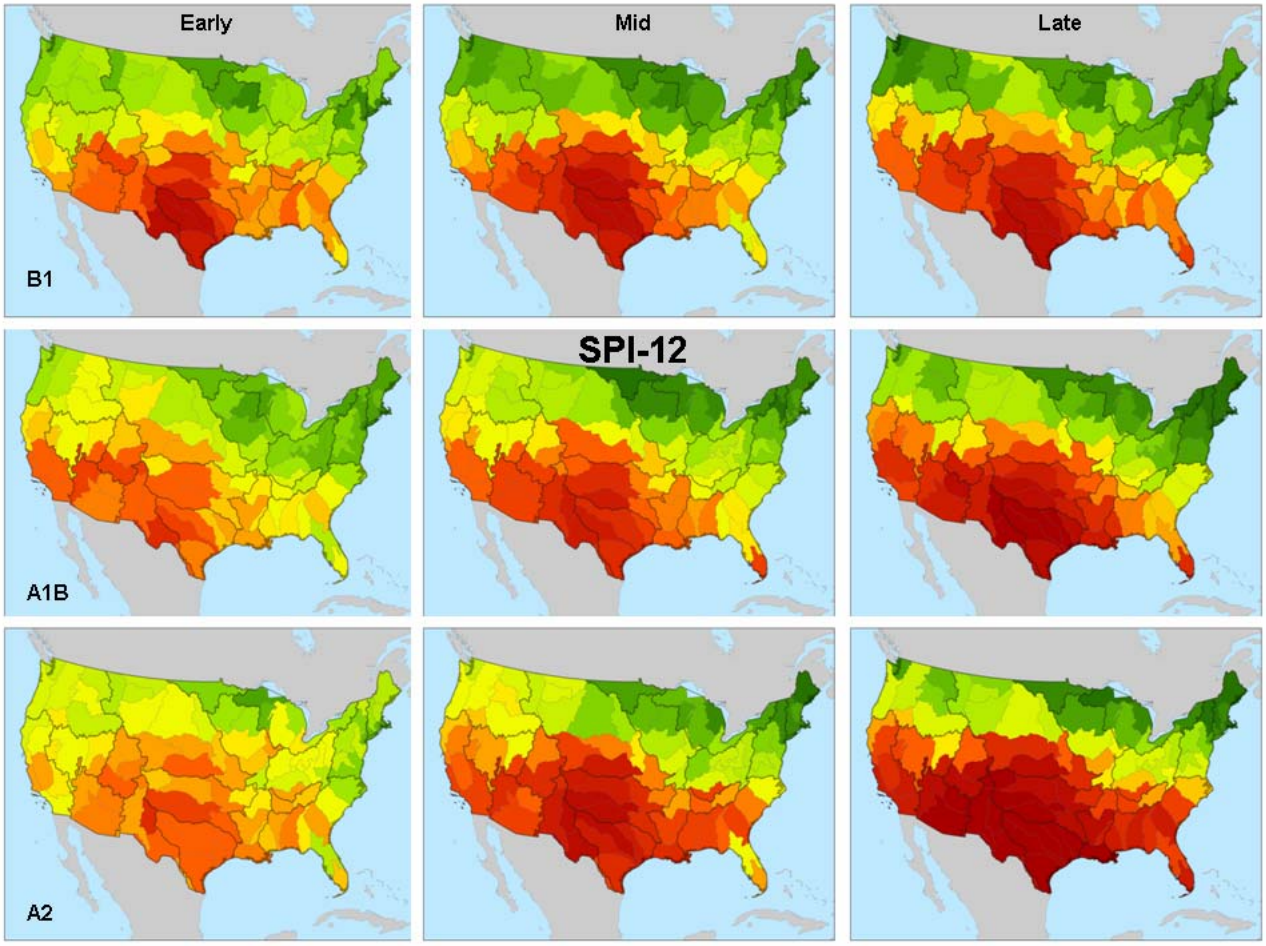

Color Scale for Figure 4, Panel B:

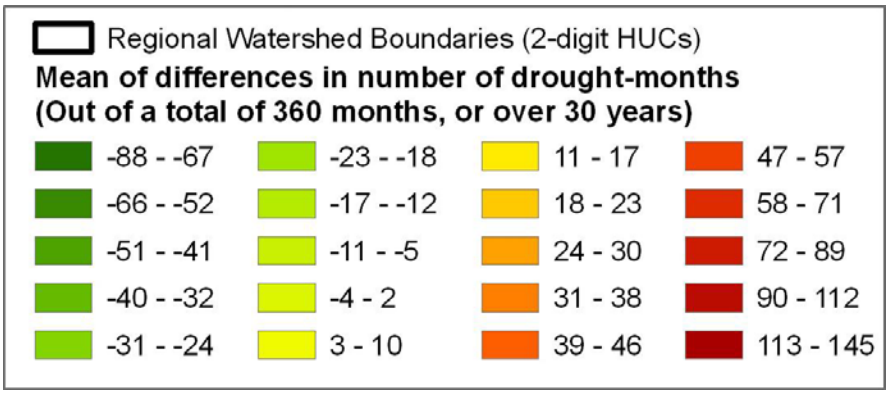

Panel C – PDSI Mild. Mean results for alternative climate scenarios.

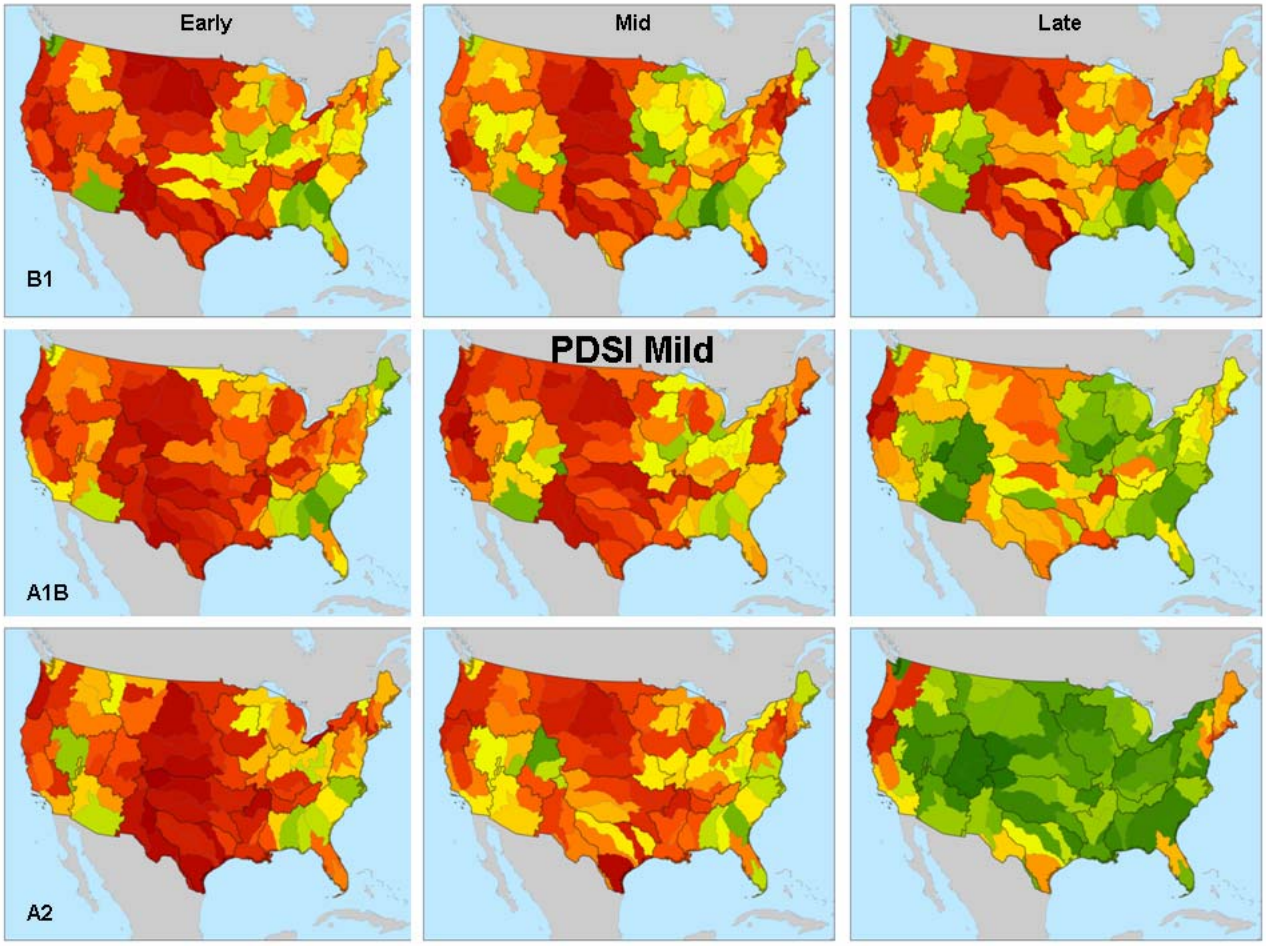

Color Scale for Figure 4, Panel C:

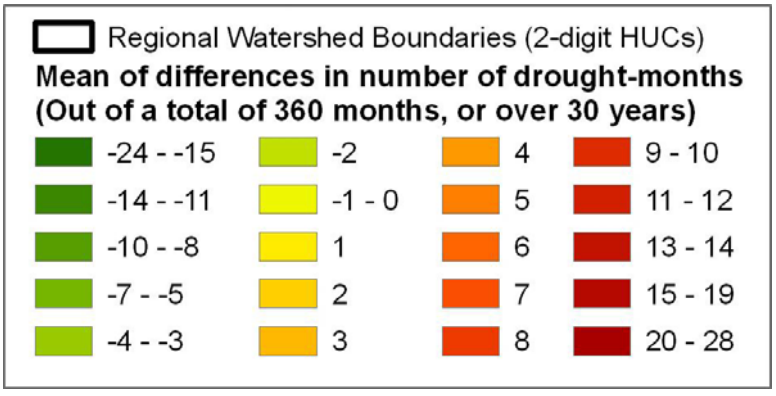

Panel D – PDSI Moderate. Mean results for alternative climate scenarios.

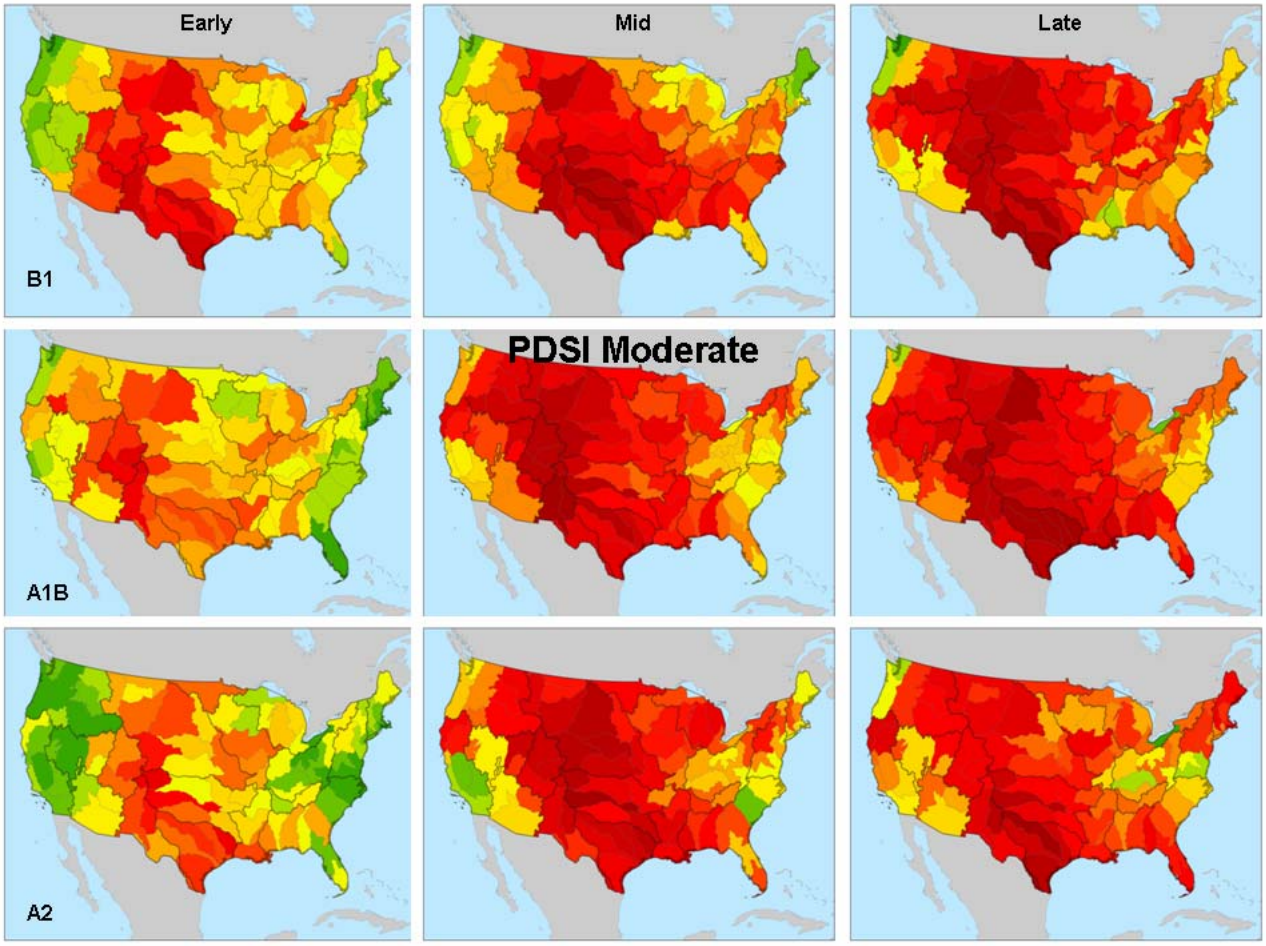

Color Scale for Figure 4, Panel D:

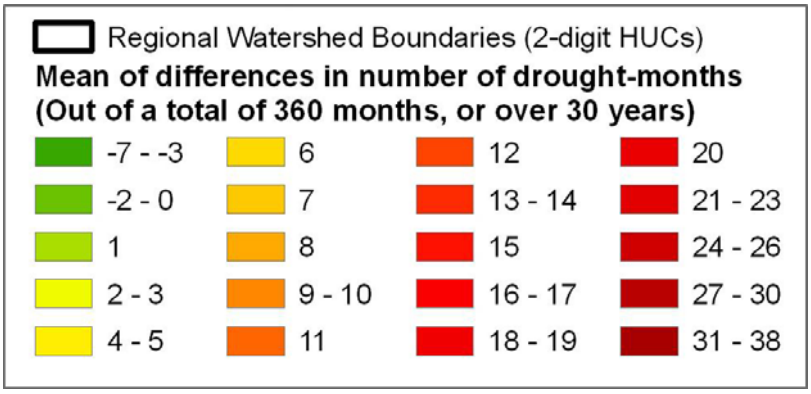

Panel E – PDSI Severe. Mean results for alternative climate scenarios.

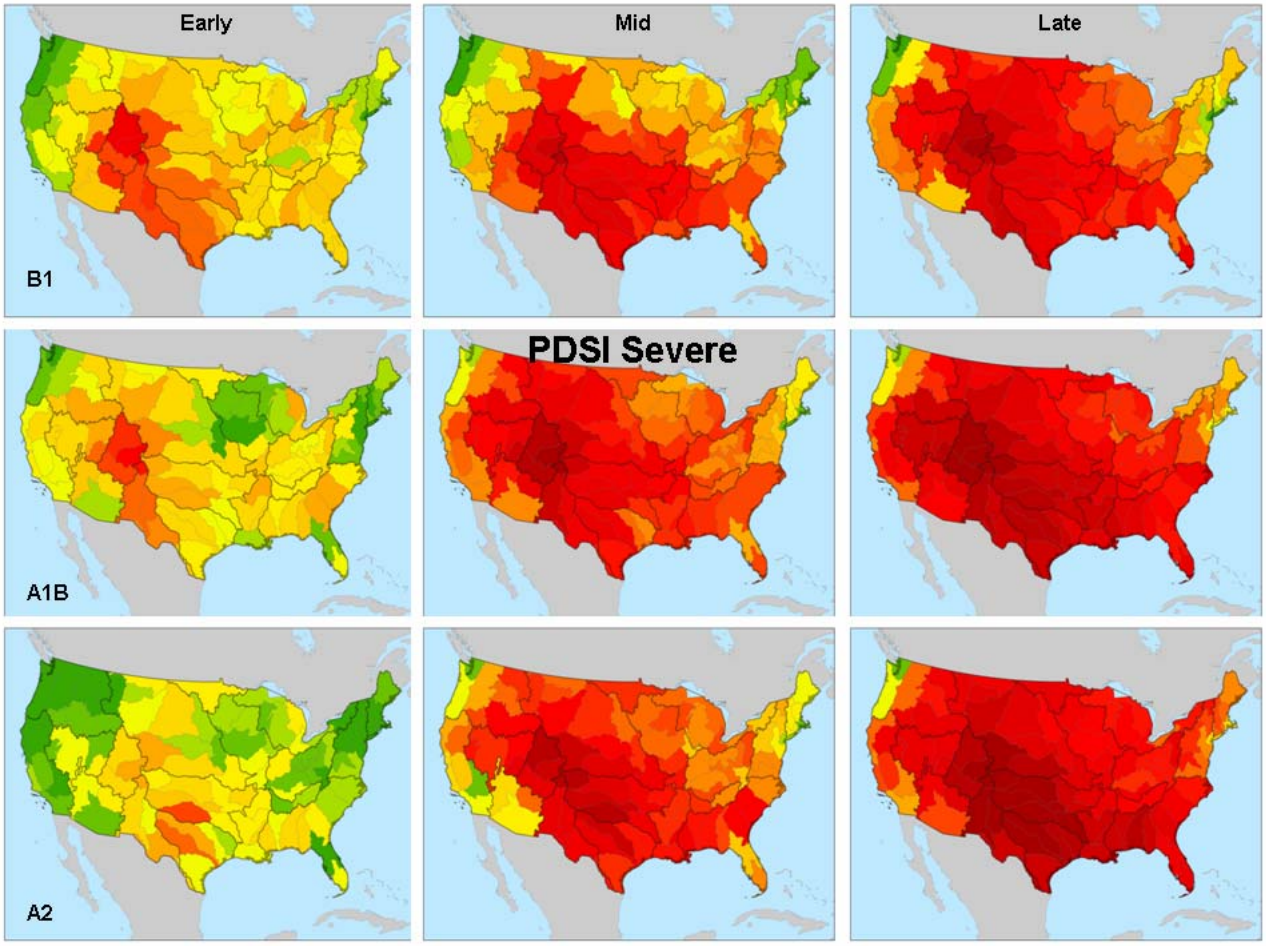

Color Scale for Figure 4, Panel E:

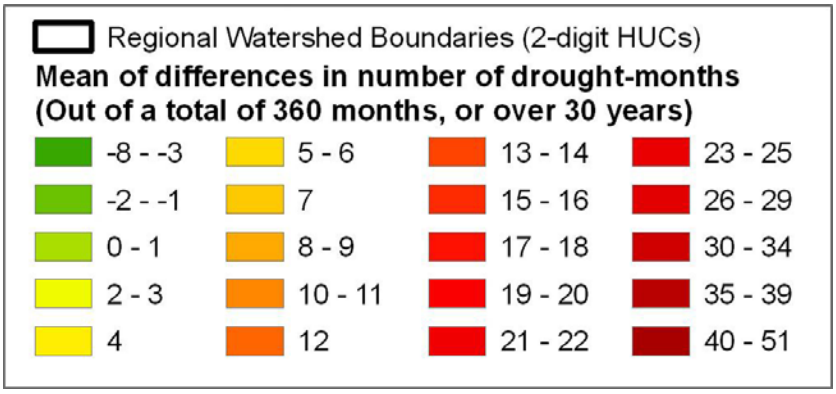

Panel F – PDSI Extreme. Mean results for alternative climate scenarios.

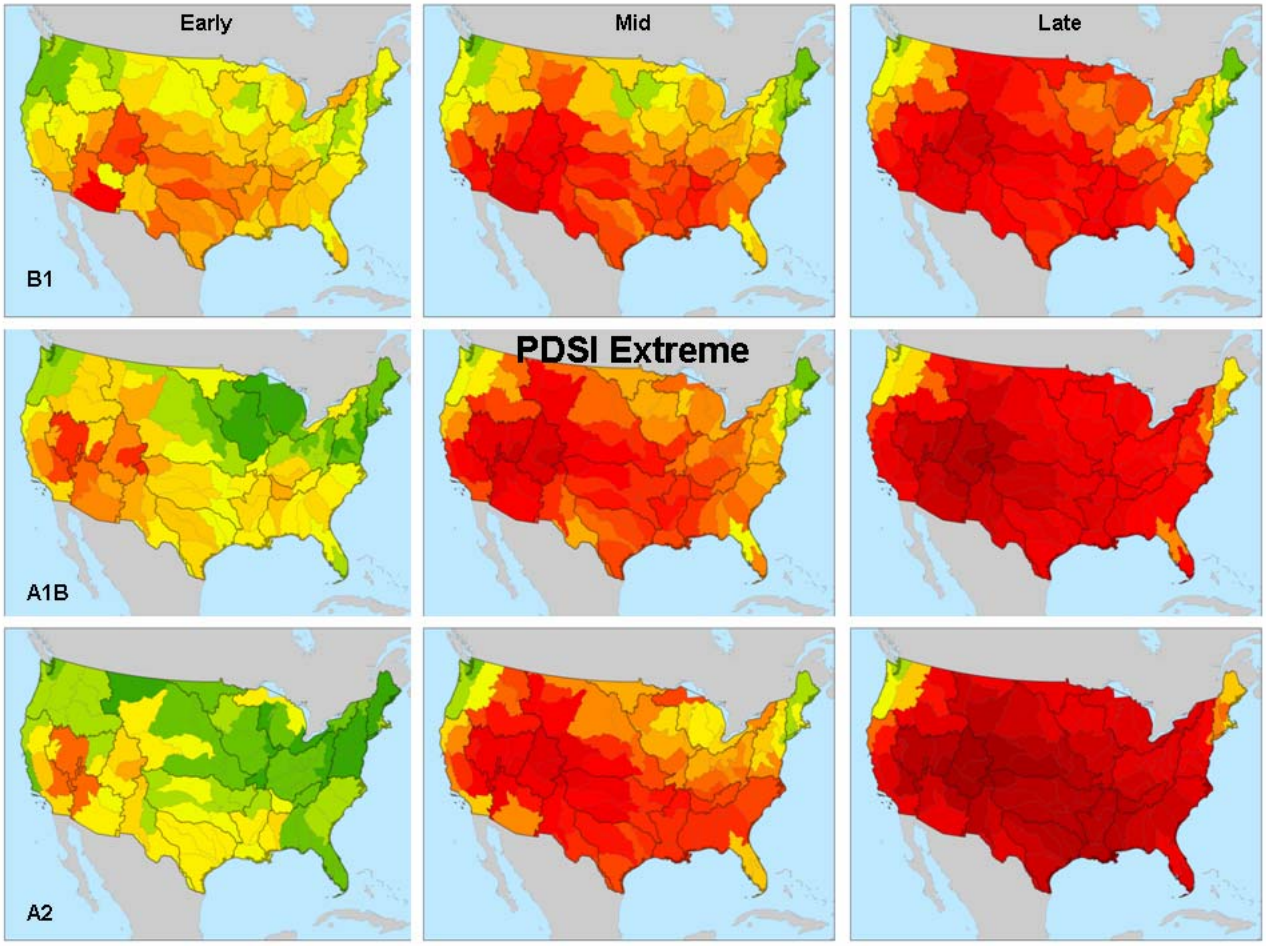

Color Scale for Figure 4, Panel F:

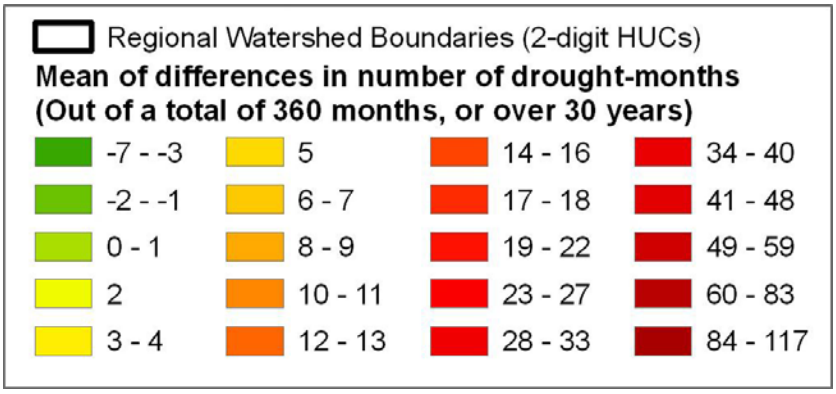

Fig. 5S The geographically distributed box and whisker diagrams for each of the 99 sub-basins for changes in the number drought months of various indices relative to the baseline for the early, middle, and late 360-month periods of this century (2006 to 2035, 2036-2065, and 2066 to 2095) for the three SRES scenarios and for the complete set of applicable GCMs. Panel A – SPI-5; Panel B – SPI-12; Panel C – PDSI mild; Panel D – PDSI moderate; Panel E – PDSI extreme; and Panel F – PDSI severe. Legend for the diagrams and calibration of the horizontal axes are indicated in Panel A.

Panel A – SPI-5. Distributions across GCMs for alternative climate scenarios.

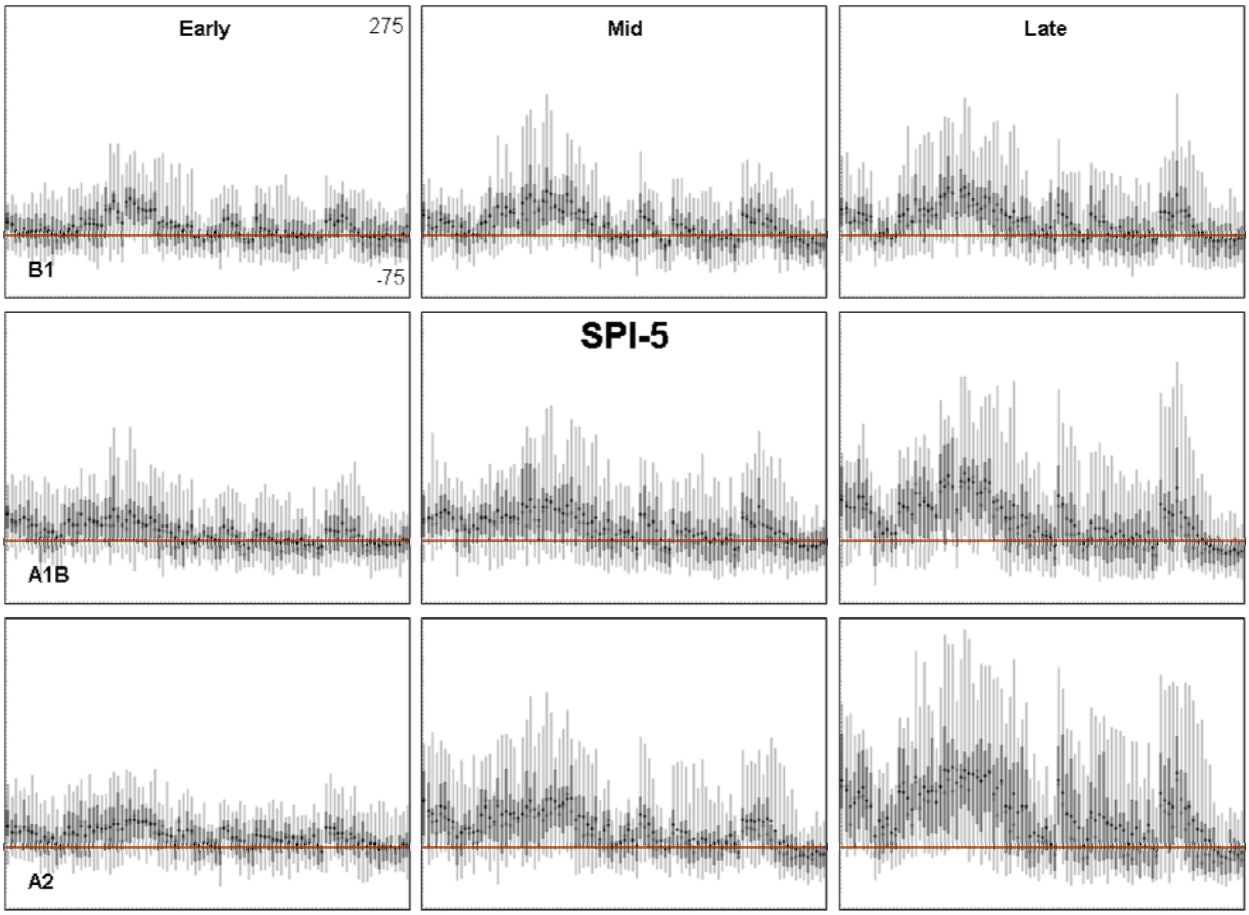

Calibration for the 99 Sub-basins for Figure 5S:

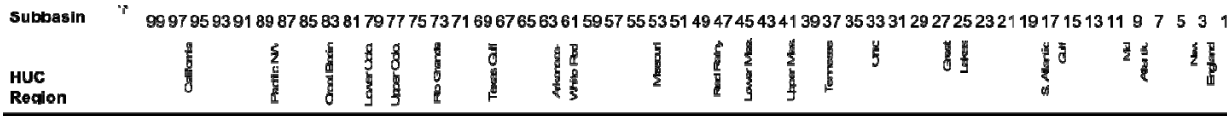

Panel B – SPI-12. Distributions across GCMs for alternative climate scenarios; scale per Panel A:

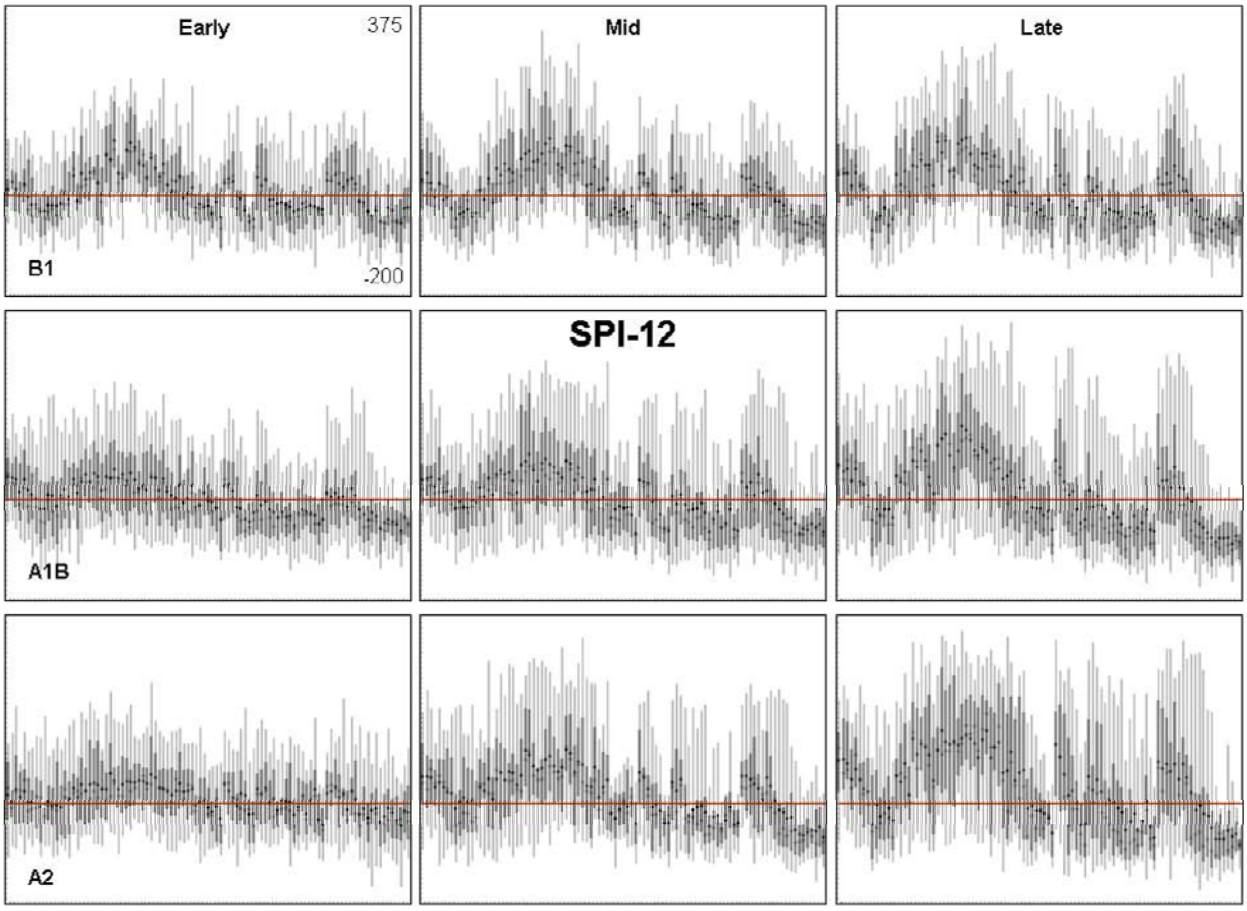

Panel C – PDSI Mild. Distributions across GCMs for alternative climate scenarios; scale per Panel A:

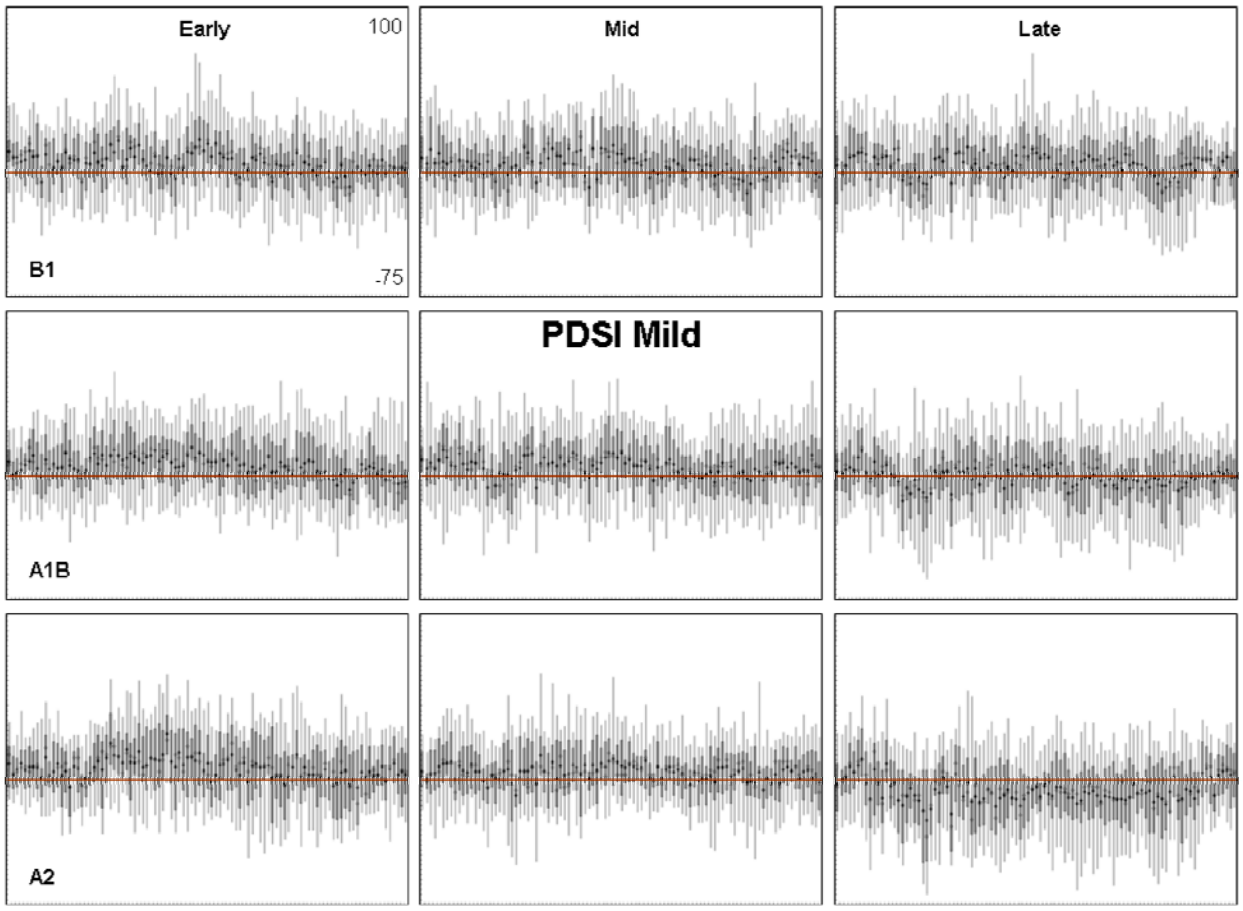

Panel D – PDSI Moderate. Distributions across GCMs for alternative climate scenarios; scale per Panel A:

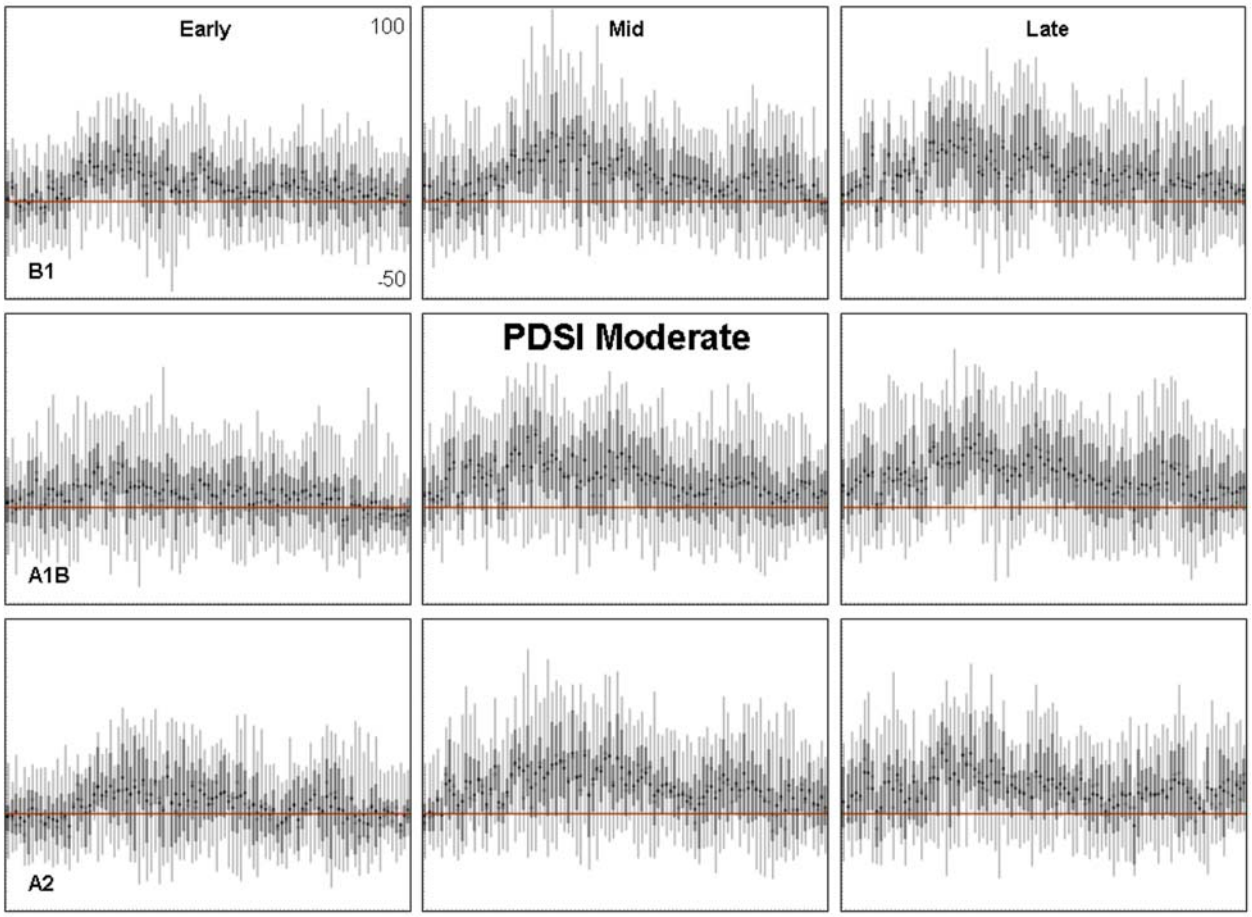

Panel E – PDSI Extreme. Distributions across GCMs for alternative climate scenarios; scale per Panel A:

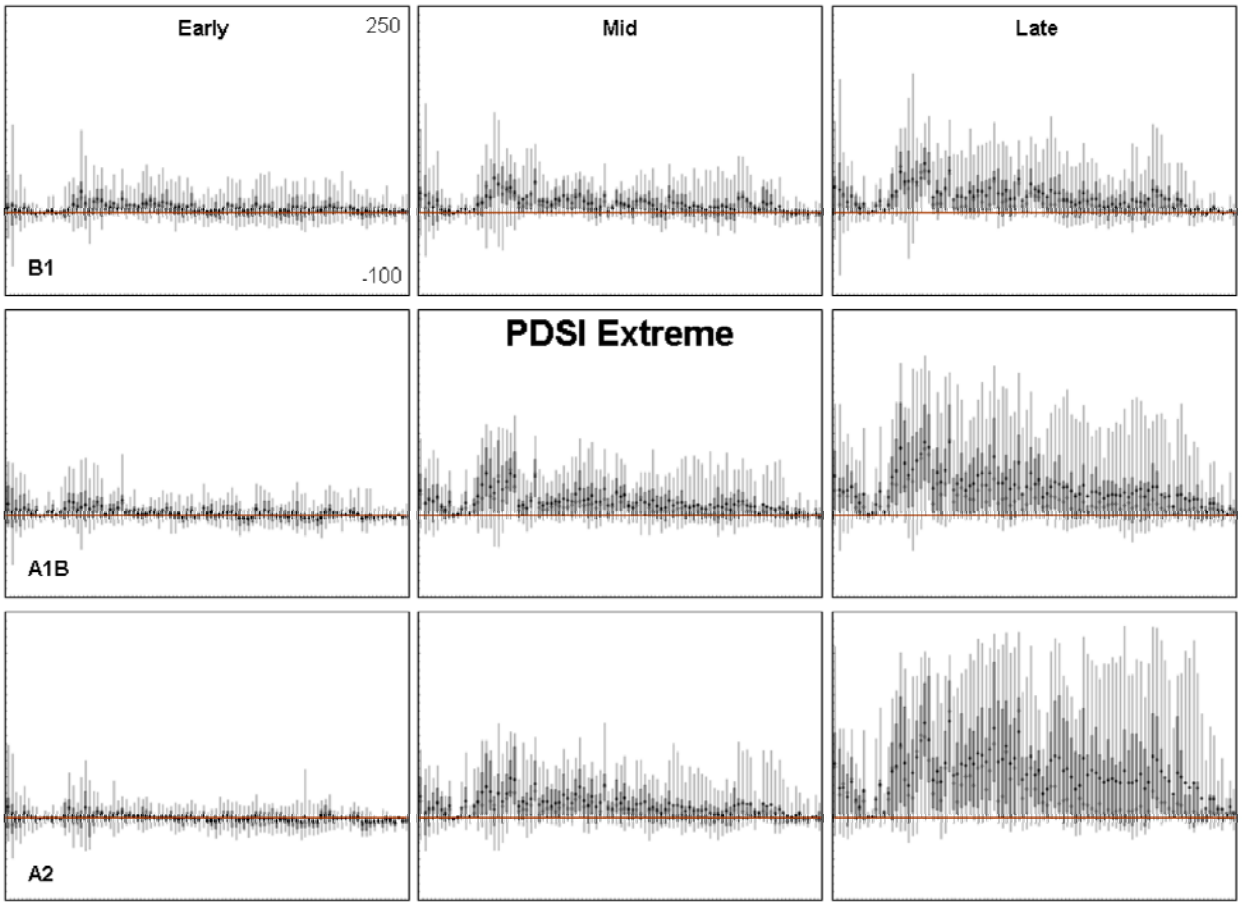

Panel F – PDSI Severe. Distributions across GCMs for alternative climate scenarios; scale per Panel A:

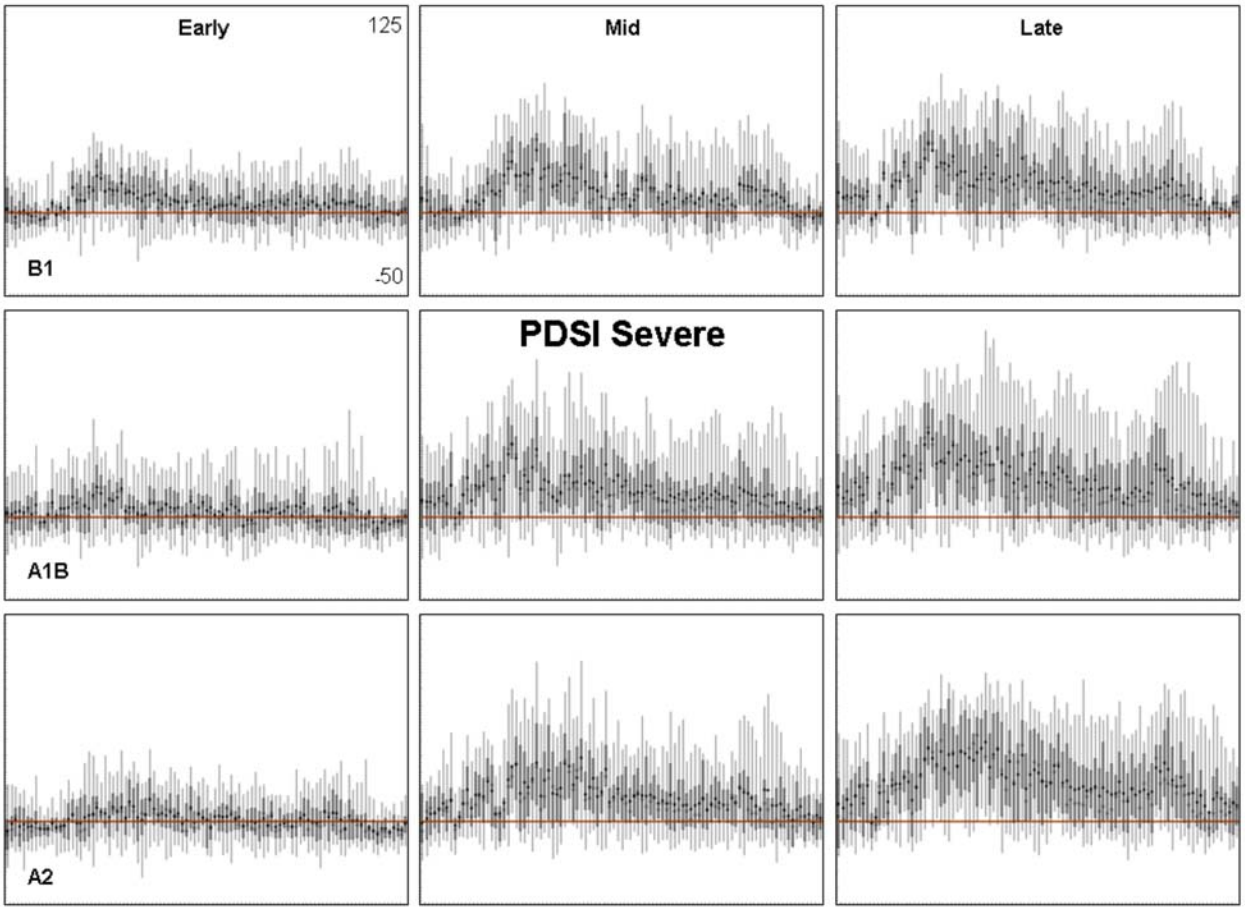

Fig. 6S An example of using sub-basin disaggregation to suggest important patterns in the relative frequencies of various levels of drought. Mean PDSI drought months are plotted for historical baseline as well as the early, middle and late 21st century time slices for the San Joaquin Valley along the three SRES emissions alternatives. Notice the increase in frequency of extreme and severe droughts at the end of the century.

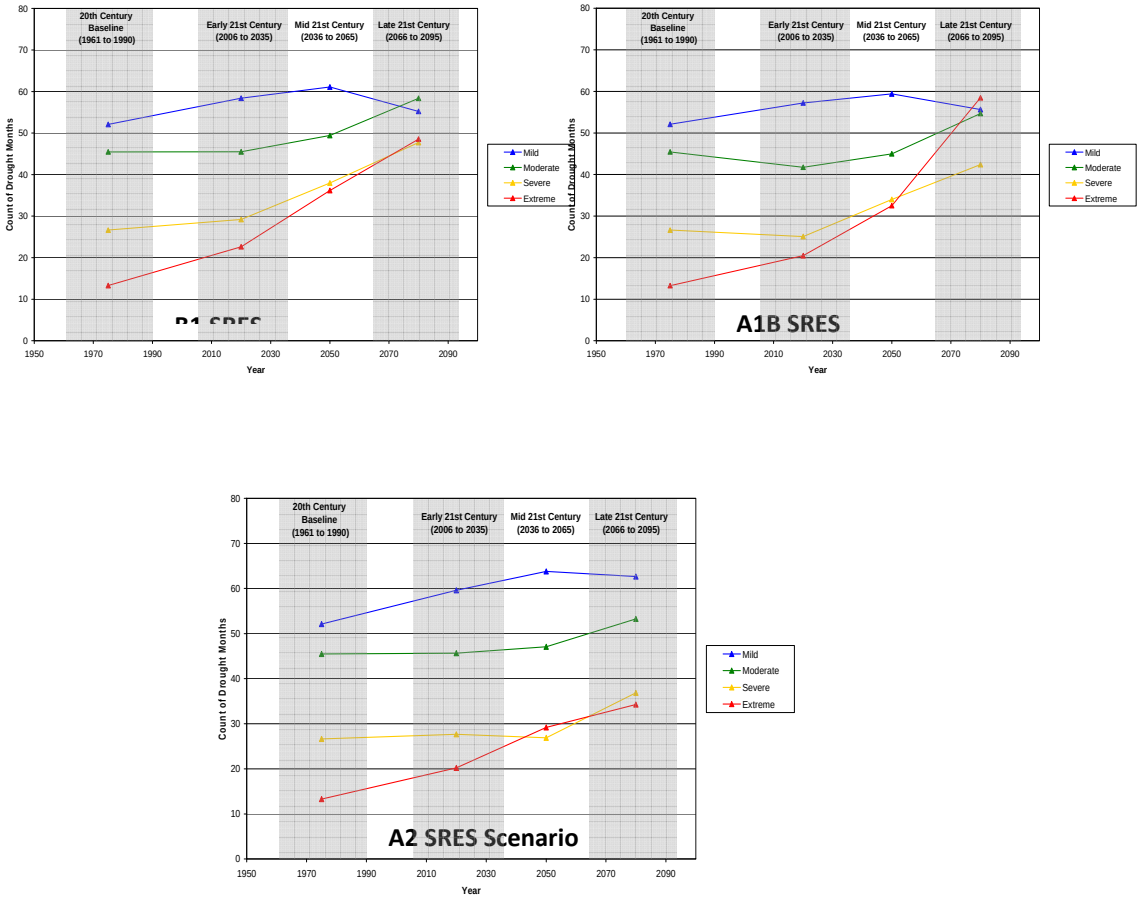

Fig. 7S Reservoir yield is the amount of water that can be sustainably supplied by a reservoir each year. On the other hand, basin yield is the water volume that can be supplied annually by all reservoirs in a basin. Basin yield can never exceed the mean annual runoff because systematic withdrawals exceeding MAR would deplete storage and eventually be impossible to sustain. The relationship between storage volume and basin yield is given by the storage-yield curve, which provides the storage capacity that is needed to provide a given firm basin yield, or alternatively, the firm basin yield that is produced from a given level of storage. Unlike runoff, reservoir yield provides information on the variability or accessibility for water supply needs rather than annual availability alone [2&3]. In Fig. 7, typical storage-yield curves are shown for a hypothetical basin. The blue line shows the storage-yield curve given the mean annual runoff (inflow) indicated by the dotted blue line. Climate change can alter the mean annual runoff and runoff variability in a basin, and can thereby change the shape of the storage-yield curve. For example, the red line shows a potential new storage-yield curve after climate change reduces mean annual runoff and/or increases variability of inflows. In this example, storage yield is reduced by $Y_{2005} - Y_{2050}$ due to climate change. To maintain constant yields, basin storage would need to be increased to K' [2&3].

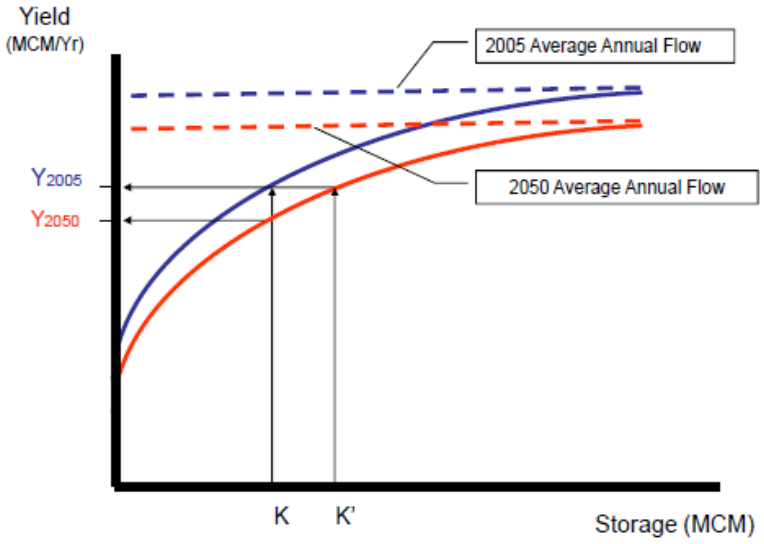

References and Notes

1 IPCC (Intergovernmental Panel on Climate Change), *IPCC Special Report on Emissions Scenarios, 4.6*, http://www.ipcc.ch/ipccreports/sres/emission/112.htm (2009).

2 World Bank. Water and climate change: understanding the risks and making climate-smart investment decisions. World Bank, Washington DC, USA (2009).

3 World Bank. The costs to developing countries of adapting to climate change: New methods and estimates: The global report of the economics of adaptation to climate change study (2009).

4 We again gratefully acknowledge the financial support of the U.S. Environmental Protection Agency's (EPA's) Office of Atmospheric Programs (Contract #GS-10F-0224J). Technical contributions and project support were provided by Jeremy Martinich, David Johnson, Caroleen Verly, and C. Adam Schlosser. Three anonymous referees offered valuable comments.